

Chapter 5

The vertical distribution of HI for 6 edge-on galaxies

P. Kamphuis ¹, R.F. Peletier ¹, and P.C. van der Kruit ¹

¹ *Kapteyn Astronomical Institute, University of Groningen, Postbus 800, 9700 AV Groningen, the Netherlands*

Abstract

THE properties of the gas in halos of galaxies constrain global models of the interstellar medium. Kinematical information is of particular interest since it is a clue to the origin of the gas. Up-to now mostly massive galaxies have been investigated for their halo properties. Here we compare the halo properties of 6 edge-on galaxies with their various other parameters. This is the first time that a sample of galaxies is compared specifically for their halo lagging properties in a consistent way. We have obtained deep HI observations for 6 galaxies and measure their lag in a consistent way and compare this to several literature studies. We find that the vertical gradient in a galaxy does not correlate with mass, Hubble type, HI scale height or 24 μm luminosity in our sample. This implies that the lags, and thus the gaseous halos, are not dominated by gas brought up from the plane through supernovae and that other origins significantly contribute.

5.1 Introduction

The discovery of a massive HI halo around NGC 891 (Swaters et al. 1997) has created a large interest in the gaseous halos of galaxies. This halo makes up $\sim 30\%$ of the total HI mass in NGC 891 and is recognized in the vertical distribution of the HI as an upward break in the vertical line profile (Oosterloo et al. 2007). It can therefore be considered an important separate component of the galaxy. Nowadays many halos have been observed and investigated in neutral and ionized gas (Schaap et al. 2000; Lee et al. 2001; Rossa & Dettmar 2003; Barbieri et al. 2005; Westmeier et al. 2005; Boomsma et al. 2005). These galaxies have mostly been investigated as individual galaxies but as yet only little attempts have been made at investigating statistical properties.

One of the most interesting things, besides its sheer size, of the halo of NGC 891 is that the gas is rotating slower above the disk (Heald et al. 2006; Oosterloo et al. 2007). This so-called 'lag' is seen as a vertical gradient in the rotation curve of $\sim 15 \text{ km s}^{-1} \text{ kpc}^{-1}$ in the neutral gas (Fraternali et al. 2005) as well as the ionized gas (Heald et al. 2006; Kamphuis et al. 2007a)

The origin of this lag has eluded theoretical explanation up to now. It is thought that most of the gas is brought up from the plane of the galaxy by galactic fountains (Shapiro & Field 1976; Bregman 1980) or chimneys (Norman & Ikeuchi 1989). Therefore, attempts have been made to explain the lag with ballistic models (Collins et al. 2002; Fraternali & Binney 2006). Even though such models can produce a lagging halo with a reasonable energy input they underestimate the observed vertical gradient (Fraternali & Binney 2006; Heald et al. 2007).

A different origin of the extra-planar gas might be from outside the galaxy. In this case the halo would be formed through the means of accretion (van der Hulst & Sancisi 1988, 2005). Since the orientation of the infalling gas is expected to be random its average angular momentum should be small. Therefore the angular momentum of the gas already in the galaxy would be lowered which could result in the vertical lag that is observed. However, to estimate the amount of infalling gas that is required to obtain the observed effect, detailed hydrodynamical modelling is necessary. Such modelling is lacking up to now.

To understand the lag observed in the halo of NGC 891 and other galaxies it is crucial to know the origin of the extra-planar gas. Even though the studies of individual galaxies has brought us a great deal of knowledge about the rotation of the extra planar gas, the origin of this gas is still a puzzle. To get a better handle on this one could, besides studying the distribution and kinematics of gaseous halos in individual galaxies in great detail, obtain a sample of galaxies with a lagging halo. With such a sample correlations between the lag and other properties of a galaxy, such as mass, star formation rate (SFR), gas mass and the vertical distribution could be studied.

If the gaseous halos are created by galactic fountains or chimneys then the size of a halo and the vertical gradient should be correlated with the overall star formation rate in a galaxy. This because the star formation rate determines the supernovae rate in a galaxy since supernovae are created by young, short lived stars. However, if some other process lies at the base of these gaseous halos a correlation between other properties, such as mass, can provide us with clues to which process this could be.

An initial attempt is made by Rossa & Dettmar (2003). They have observed 74 galaxies in $\text{H}\alpha$ to determine the frequency of extra planar diffuse ionized gas (eDIG)

emission. They found that $\sim 40\%$ of edge-on galaxies reveal an extra planar component of ionized gas. In their sample the eDIG is correlated with the SFR of the galaxies which indicates an internal origin for this gas. However, since they only have imaging observations and no kinematics this gas might also be partially in line-of sight warps or flares. Also, it is unclear whether this gas is lagging or co-rotating.

Heald et al. (2007) have investigated three galaxies (NGC 4203, NGC 891, NGC 5775) where a lag has been found in the ionized gas. They investigated the correlation of the lag with the scale height and found that this is approximately constant $\sim 15\text{-}25 \text{ km s}^{-1} \text{ kpc}^{-1}$ per electron scale height. However, these galaxies are all very similar except in their SFR and therefore a correlation with other parameters could not be investigated.

Since the halo has a low surface brightness it is necessary to obtain extremely sensitive observations to analyze its kinematics. Not many edge-on galaxies have been observed to the required depth in HI nor H α . Even though nowadays there are several galaxies with indications of a lagging halo, with the exception of NGC 891, NGC 4302 and NGC 5775 no vertical gradient has been quantified. Even more, this lag has been quantified in HI only for NGC 891.

In this Chapter we will select a sample of edge-on galaxies that are nearby, isolated and edge-on. Of primary importance is that the sample has a range in star formation properties and mass. These galaxies will be modelled in a systematic way. Modelling the galaxies for different lags enables us to obtain the lag in a galaxy by measuring the gradient in normalized PV- diagrams in the data as well as the models. This comparison between the models and the data is necessary to obtain a lag because beam smearing and partial line-of-sight warps can introduce apparent lags.

With the obtained lags, or lack of halo, we will then look for correlations between the lag and other properties of the galaxies such as mass, HI mass, scale height and SFR.

This Chapter is structured as follows. In § 5.2 we will present the data and the criteria used for the selection of a sample. In § 5.3 the modelling and the method of analysis will be discussed. The results will be presented and discussed in § 5.4 and in § 5.5 we will summarize and discuss Future Work.

5.2 Data and Sample selection

As mentioned in the introduction we have selected a set of nearby, isolated edge-on galaxies. Because we will study the galaxies in HI, where the resolution is often $> 10''$ the galaxies have to be nearby. To detect the faint outer parts of the vertical distribution, an edge-on orientation is preferred. Also, we are not interested in gas brought up from the plane through the interaction with other galaxies and therefore the galaxies in the sample should be isolated.

Since we are interested in very faint 21 cm emission we also would like the galaxies to be observable with the Very Large Array (VLA) and the Westerbork Radio Synthesis Telescope (WRST). Therefore the galaxies should be in the Northern Hemisphere and above 20° declination. To ensure these criteria we have taken the following steps.

From the UGC (Uppsala Galaxy Catalogue) we have selected the galaxies that are classified as highly inclined (UGC class 7) and have a declination above 20° . Through a visual inspection of the optical photographs and previous work we ensure that all the galaxies indeed have an inclination $\geq 85^\circ$. To this sample of 14 nearby edge-on spiral

UGC No.	Alt. name	RA (J2000)	DEC (J2000)	Reference
UGC 0008	NGC 7814	00 ^h 03 ^m 15 ^s	16°08' 43.5''	Kamphuis et al. (2007b)
UGC 1281		01 ^h 49 ^m 32 ^s	32°35' 24''	This thesis, Chapter 4
UGC 1831	NGC 891	02 ^h 22 ^m 33 ^s	42°20' 52''	Oosterloo et al. (2007)
UGC 4704		08 ^h 59 ^m 00 ^s	39°12' 36''	Swaters (1999)
UGC 7321		12 ^h 17 ^m 34 ^s	22°32' 25''	Matthews & Wood (2003)
UGC 7774		12 ^h 36 ^m 23 ^s	40°00' 18''	Swaters (1999)

Table 5.1: The sample, their positions and original publications

UGC No.	Type	PA °	Distance Mpc	v_{hel} km s ⁻¹	v_{max} km s ⁻¹	D ₂₅ '
UGC 0008	Sab	135	16.4	1044	220	5.5
UGC 1281	Sdm	38	5.4	156	60	4.4
UGC 1831	Sb	22	9.5	528	220	13.5
UGC 4704	Sdm	115	8.0	596	50	4.1
UGC 7321	Sd	82	5.24	408	110	5.5
UGC 7774	Sc	102	7.8	526	100	3.6

Table 5.2: Global parameters of the sample. PA, type and D₂₅ from RC3 (de Vaucouleurs et al. 1992). Distance from the NASA extra galactic database. v_{hel} and v_{max} from this work (See § 5.3)

galaxies two additional galaxies are added, NGC 7814 (which has low declination but is large enough to be observed) and UGC 7774 (which has UGC class 6 but has 85° inclination). The diameters of these galaxies range from 3'.6 to 16'.6 in D₂₅ (Table 5.2).

We obtained deep HI observations ($\sigma < 1$ mJy) for 6 of these 16 galaxies. Of these observations 2 are new observations with the WRST (NGC 7814 and UGC 128; Kamphuis et al. (2007b)) and 4 are archival data (NGC 891; Oosterloo et al. (2007), UGC 4704 and UGC 7774; Swaters (1999), UGC 7321; Matthews & Wood (2003)). These galaxies are presented in Table 5.1.

Of the six galaxies in the sample only NGC 891 and NGC 7814 have NGC numbers; therefore we will refer to these galaxies by their UGC number as well. These numbers are UGC 1831 and UGC 0008 respectively.

Even though this sample is small it covers a wide range of morphologies, masses and SFRs (See Table 5.2 and 5.3).

5.3 Modelling

We modelled the galaxies with the Tilted Ring Fitting Code (Józsa et al. 2007) TiRiFiC. TiRiFiC fits a tilted ring model to the HI data cubes through the means of χ^2 minimization. Most studies in the literature determine the best fit by eye. Using the new TiRiFiC models is a great step forward from comparing the models by eye, but it is by no means the holy grail of finding the correct model. Since there are parameters

UGC No.	L $24 \mu\text{m}$ $\times 10^{20} \text{ erg s}^{-1} \text{ Hz}^{-1}$	F $\text{H}\alpha$ $\times 10^{-13} \text{ erg s}^{-1} \text{ cm}^{-2}$	L $\text{H}\alpha$ $\times 10^{39} \text{ erg s}^{-1}$	SFR $\text{H}\alpha$ $\text{M}_{\odot} \text{ yr}^{-1}$
UGC 0008 ⁺	2.7	6	15	0.11
UGC 1281 [*]	0.4	3.8	1.148	0.009
UGC 1831	6.9	44.6	38.9	0.3
UGC 4704	-	1.3	0.95	0.0075
UGC 7321	0.07	-	-	-
UGC 7774	0.22	1.3	8.5	0.067

Table 5.3: Global SFR parameters of the sample. $24 \mu\text{m}$ luminosity derived from spitzer archival images $\text{H}\alpha$ fluxes and luminosities from Kennicutt et al. (2008).⁺ $\text{H}\alpha$ flux from Hameed & Devereux (2005). ^{*} $25 \mu\text{m}$ luminosity from the IRAS catalogues.

that are degenerate, such as inclination and scale height, some restrictions are required to obtain a good fit.

TiRiFiC fits a disk made of several rings. Even though such a tilted ring model has great freedom in the radial direction it is somewhat limited in the vertical direction. The rings in the model are described by a single exponential in the vertical direction whereas there are several examples where the observations are better described by a double exponential (See the vertical distribution of NGC 891 (Oosterloo et al. 2007)). Also, TiRiFiC does not fit a lag to the galaxy. If there is a galaxy with a lag it tries to fit this with either a flare or a line of sight warp. One can however distinguish between a lag, a flare and a warp. A flare will clearly show in the channel maps as a butterfly effect and a line of sight warp will produce outer channel maps where the intensity distribution is too wide in the vertical direction. These limitations have to be taken into account.

To avoid concluding on the wrong parameters we construct three different models for each galaxy. In first model we restrict the model in such a way that it can have only one value for the scale height and inclination for all the rings in the model. This means that the model cannot flare nor warp into the line of sight (Model A). Then we construct two models in which either the inclination can vary per ring (Model B) or where the scale height can vary per ring (Model C). This corresponds to modelling either a line of sight warp or a flaring disk.

Even though a real galaxy might be flaring as well as warping into the line of sight we do not model this option. This is because in such a model it would become very hard to determine the actual quality of the fit and thus the analysis would not give a clear answer. We do however fit the two sides of the galaxy separately to account for any asymmetries.

After obtaining a satisfying fit for the three different models we reproduce the models with a range of lags. We then measured the apparent lag of the data and the different lagging models as described in Chapter 4. This way of measuring the vertical gradient does not distinguish between a vertical gradient from a halo, a warp, or a flare. Therefore it is necessary to determine this lag in the models as well as the data if there is a warp or flare. However, in the absence of a flare or warp (Model A) and in an highly inclined disk, like in UGC 1831, this measurement gives the vertical gradient of the rotation curve directly and is actually more reliable than a comparison to the model since the model

UGC No.	Best Fit Model	vertical gradient in max rot velocity ($\text{km s}^{-1} \text{kpc}^{-1}$)
UGC 0008	Model A	0 ± 0
UGC 1281	Model B	0 ± 8.4
UGC 1831	Model A	13.9 ± 3.0
UGC 4704	Model A	5.3 ± 0.8
UGC 7321	Model A	15.8 ± 4.4
UGC 7774	Model B	0 ± 0

Table 5.4: Best fit models and their lag. Model A is a model without flaring and without a line of sight warp, Model B contains a line of sight warp, Model C is a flaring model.

will always contain small deviations from the actual distribution of HI.

After having measured the lag for all the models we compare the best fit models with a lag and without a lag to the data cube to see which provides the better fit. Also, at this stage we will determine whether Model A, B, or C is the better model for each galaxy. Table 5.4 shows the lag measurement plus the best fit model for each of our six galaxies.

5.3.1 Notes on individual models

Here, we give a description of the models per galaxy individually and document why we prefer one model over the other. The channel maps of each galaxy overlaid with contours of the best fit model can be found in the color appendix in the back of this thesis.

UGC 0008

Figure 5.1 shows the parameters of the best fit models for UGC 0008. For this galaxy all three models fit the data evenly well. The vertical extent of the data is too small to be measured due to beam smearing. Therefore, it is also impossible to measure any lag. If any lag or even extra-planar gas is present in this galaxy it is completely obscured by beam smearing. A visual inspection of the models shows that also by eye it is impossible to distinguish between the different models. Therefore we assume the simplest model, with no lag, no flare and a constant inclination (Model A).

UGC 1281

From the detailed analysis in Chapter 4 we have already seen that this galaxy is fitted equally well by a line of sight warp and a vertical lag of $8.7 \pm 4.1 \text{ km s}^{-1} \text{kpc}^{-1}$. However, in that chapter the fit was done by eye. Here we include the same analysis for UGC 1281 as the rest of the sample.

For UGC 1281 all the models are inconsistent with a non-lagging halo (See bottom right Panels in Fig 5.2). However, for Model B, a line of sight warp, this inconsistency is only $0.3 \text{ km s}^{-1} \text{kpc}^{-1}$ at the lower limit. The fact that for our fitting in this chapter

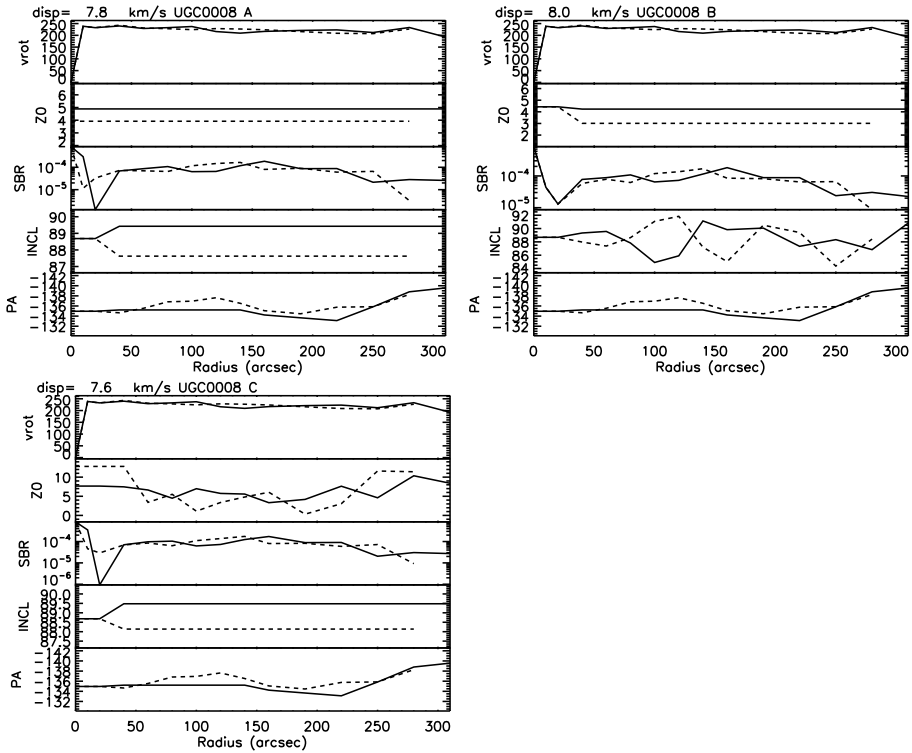


Figure 5.1: Top left panel: the parameters for the best fit non-flaring model without a line of sight warp (Model A) for UGC 0008. From top to bottom these parameters are: the rotational velocity (vrot), the scale height (z_0), the surface brightness (SBR), the inclination (INCL), and the position angle (PA) for each ring. The parameters are plotted against radius in arcsec. The top right panel and the bottom left panel show the parameters for the best fit line of sight model (Model B) and the best fit flaring model (Model C) for this galaxy.

a line of sight warp is excluded is caused by the fact that we do not combine the warp with a flare.

From a visual comparison between the data and the models we find that indeed non-lagging models are inconsistent with the data. We also find that a flaring model with a lag (Model C, $\text{lag}=8.3 \text{ km s}^{-1} \text{ kpc}^{-1}$) produces too much flux above the plane at large radii. We are not able to separate between a lagging halo (Model A, $\text{lag}=6.4 \text{ km s}^{-1} \text{ kpc}^{-1}$) or a line of sight warp (Model B, $\text{lag}=0, 7.7 \text{ km s}^{-1} \text{ kpc}^{-1}$), whether it is lagging or not.

As we have already seen in the detailed analysis of UGC 1281 (Chapter 4) such an analysis leads to the same conclusion. Therefore, we revert to the conclusion of our previous Chapter and assume for the lag of UGC 1281 a range of $0\text{-}8.7 \text{ km s}^{-1} \text{ kpc}^{-1}$. Figure 5.2 shows the parameters for each model.

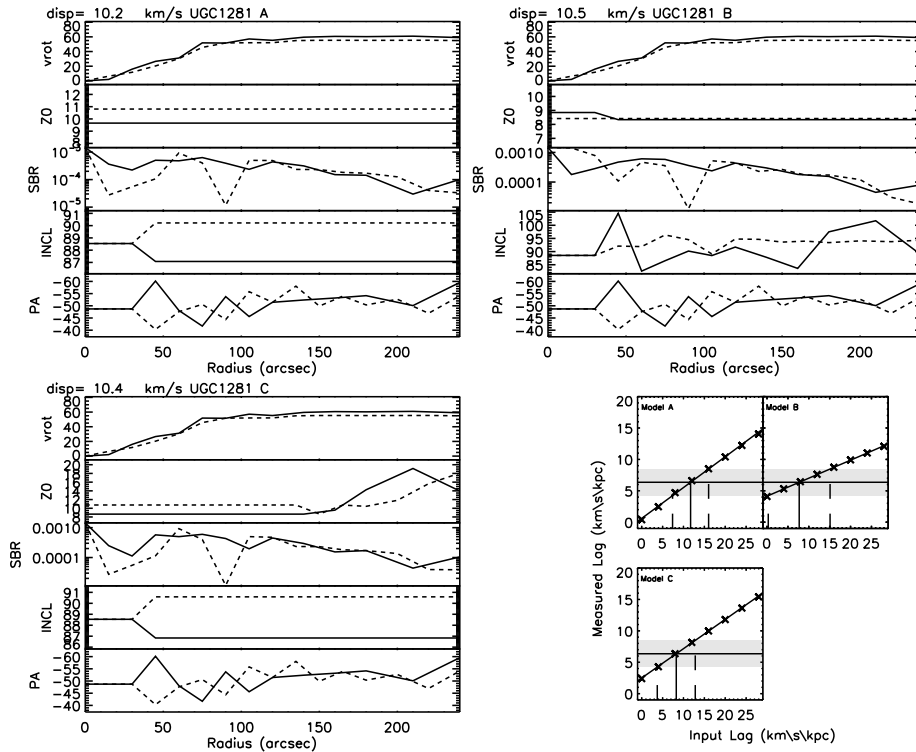


Figure 5.2: As Figure 5.1 but for UGC 1281. The additional three little panels in the bottom right show the fits to normalized PV-diagrams of the data and the best fit models with a range of lags (See Chapter 4, §4.4.2) in the same arrangement as the parameter panels (e.g. Top left Model A, Top right Model B, Bottom left Model C).

UGC 1831

UGC 1831 is known to have a halo that is lagging (Swaters et al. 1997; Oosterloo et al. 2007). This galaxy can therefore be used as a reference frame for the analysis in this Chapter. This galaxy is best fit in the vertical direction by two exponentials (See figure 5.15, middle left panel). Here there is a problem as TiRiFiC tries to fit the brighter inner disk whereas we are interested in the outer vertical component.

When we compare our three best fit models with the data we see that all of them indeed severely underestimate the scale height of UGC 1831. An investigation of the channel maps shows us that the basic shapes of Model B and C are completely off (See Figure 5.3). Model B (Green Contours) which resembles the line of sight warp produces channel maps that blow up in the vertical direction at radii the furthest removed from the center of the galaxy. This is indicated by the green arrows in Figure 5.3. Model C (yellow contours) shows channel maps with a clear V shape (yellow arrows). Both these shapes cannot be recognized in the data and we therefore conclude that Model A is the best fit to the data.

When we look at the top panels of Figure 5.4 we see only small differences between

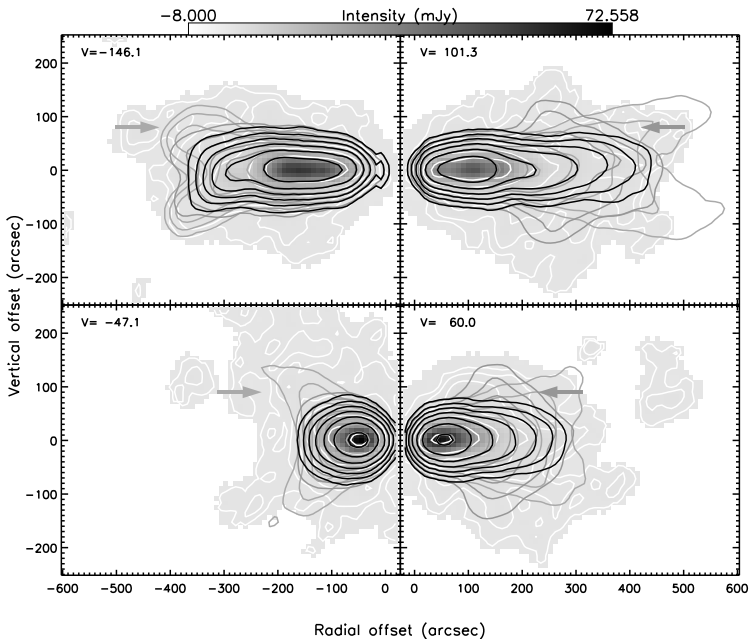


Figure 5.3: Four channel maps of UGC 1831. The velocities relative to the systemic velocity are shown in the top left corner of each panel. The color map and the white contours are the data. The red contours show the best fit model (Model A) with a lag of $13.9 \text{ km s}^{-1} \text{ kpc}^{-1}$. Green contours are show the line of sight model (Model B) with a lag of $20 \text{ km s}^{-1} \text{ kpc}^{-1}$. Yellow contours are the flaring model with a lag of $16 \text{ km s}^{-1} \text{ kpc}^{-1}$. Contour levels are 1σ , 3σ , 7.5σ 18.75σ etc. ($\sigma = 0.2 \text{ mJy}$). The green and yellow arrows indicate where the shape of the models deviates from the shape of the data (See text). Color version on Page 139.

parameters of model A (left panel) and model B (right panel). This again indicates that great care must be taken in the modeling since Figure 5.3 clearly shows that these parameters result in very different models.

If the only difference between the second vertical component and the bright inner disk is the scale height the lag should still be measured correctly in our models. When we look at the bottom right panels of Figure 5.4 we see this is not the case. Only for the line of sight warp (Model B, top right panel of the little panels in Fig. 5.4) is the obtained input value consistent with the lag obtained for this halo in the literature (Fraternali et al. 2005; Heald et al. 2006). The fact that our comparison between measured lag and input lag in Model A and Model C (Top left little panel, bottom little panel respectively in Fig. 5.4) is inconsistent with the literature is caused by the fact that TiRiFiC tries to fit the double exponential vertical profile with a single exponential. However, in the absence of a warp and no significant flaring (Model A) the lag can be measured directly from the data. This gives us a lag for UGC 1831 of $13.9 \pm 3.0 \text{ km s}^{-1} \text{ kpc}^{-1}$ which is consistent with the literature.

Oosterloo et al. (2007) have modeled this galaxy with a two disk model, thus properly resembling the the double exponential in the vertical distribution. They find that the lag in the halo of this galaxy is best fitted by a vertical gradient of $15 \text{ km s}^{-1} \text{ kpc}^{-1}$ which is consistent with our results.

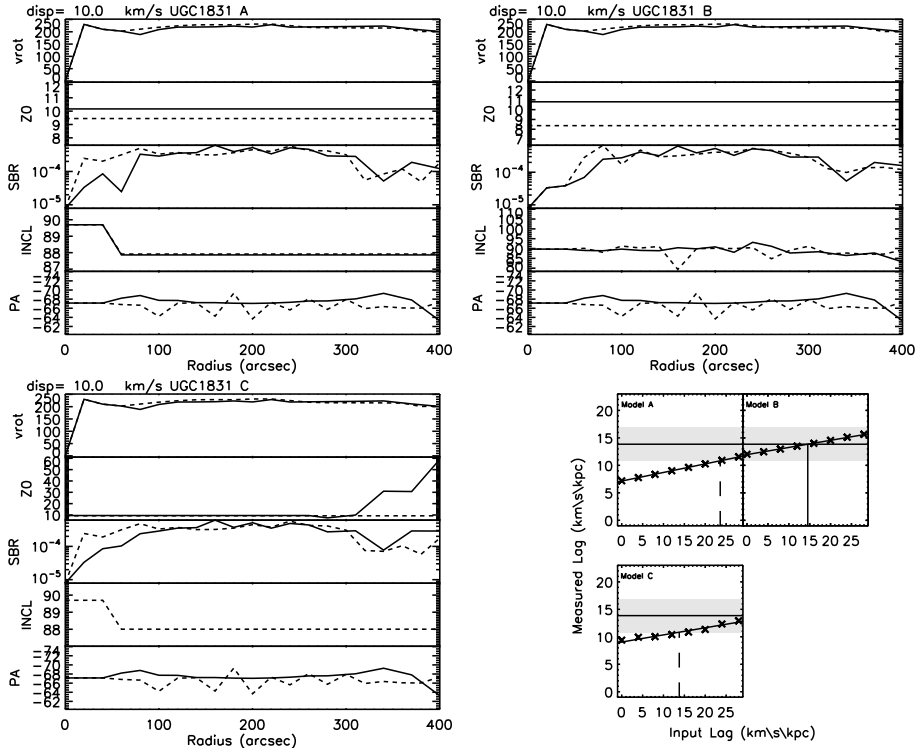


Figure 5.4: Same as Fig. 5.2 but for UGC 1831

UGC 4704

For UGC 4704 there is not much difference between the three models. Figure 5.5 shows for channel maps of the data overlaid with the contours of the three models. From these channel maps we see that it is impossible to distinguish between model A and B (red and green contours respectively). There is a hint on the approaching side of the galaxy that Model C (yellow contours) produces too much intensity above the plane at large radii at the receding side of the galaxy, but this is only seen in the 1σ contour and cannot be called significant. This deviation from the data is indicated in Figure 5.5 by the black arrows in the left panels.

All the vertical gradient measurements for UGC 4704 are inconsistent with a non-lagging distribution (See Figure 5.7, the little panels in the bottom right corner). When we look at the Position Velocity (PV) diagrams parallel to the major axis above and below the plane we can confirm that a lagging model provides the better fit. Figure 5.6

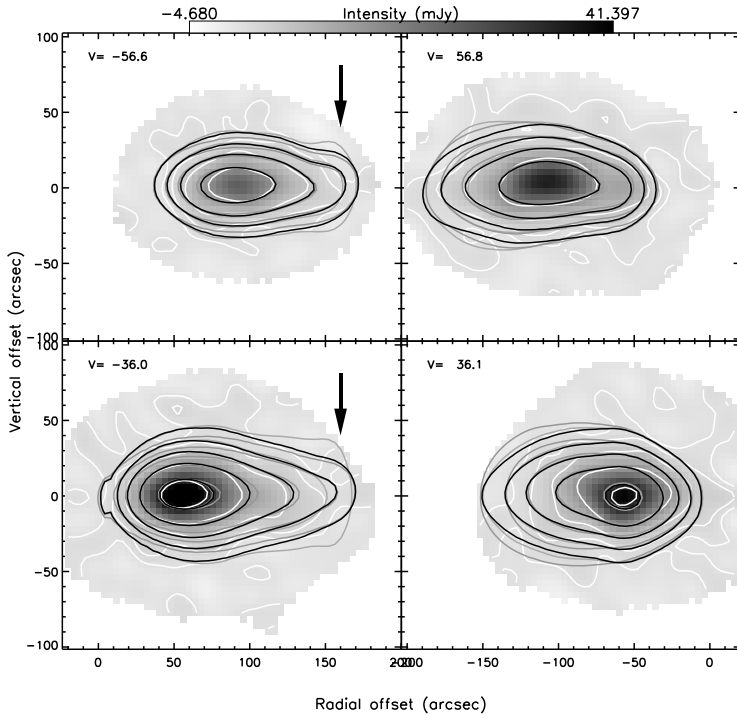


Figure 5.5: Four channel maps of UGC 4704. The velocities relative to the systemic velocity are shown in the top left corner of each panel. The color map and the white contours are the data. The red contours show the best fit model Model A with a lag = $5.3 \pm 0.8 \text{ km s}^{-1} \text{ kpc}^{-1}$. Green contours show the line of sight warp (Model B) with a lag of $8 \text{ km s}^{-1} \text{ kpc}^{-1}$. Yellow contours are the flaring model (Model C) with a lag of $4 \text{ km s}^{-1} \text{ kpc}^{-1}$. With contour levels 1σ , 3σ , 7.5σ , 18.75σ etc. ($\sigma = 0.78 \text{ mJy}$). The black arrows indicate where the flaring model deviates from the data. Color version on Page 140.

shows two of such PV diagrams averaged over the range from 30 to $40''$ above and below the plane. Here the contours of Model A are overlaid on the data with the white contours showing a model with a vertical gradient of $5.3 \text{ km s}^{-1} \text{ kpc}^{-1}$ and the red contours a model without a vertical gradient. If we compare the non lagging best fit line of sight warp model (Model B) and the best fit non lagging flaring model (Model C) to their models with a lag we see that the lagging model is also a better fit in these cases. This is not surprising since the parameters of the different model do not differ much. This is easily seen in Figure 5.7 which shows the parameters in the top panels and the bottom right panel.

We therefore conclude that this galaxy is best fit with a disk that has no line of sight warp and no flare (Model A). As we have seen in UGC 1831 TiRiFiC tries to compensate for a lag by adjusting the parameters in the best fit model. We therefore assume a lag of $5.3 \pm 0.8 \text{ km s}^{-1} \text{ kpc}^{-1}$ which is directly measured from the data.

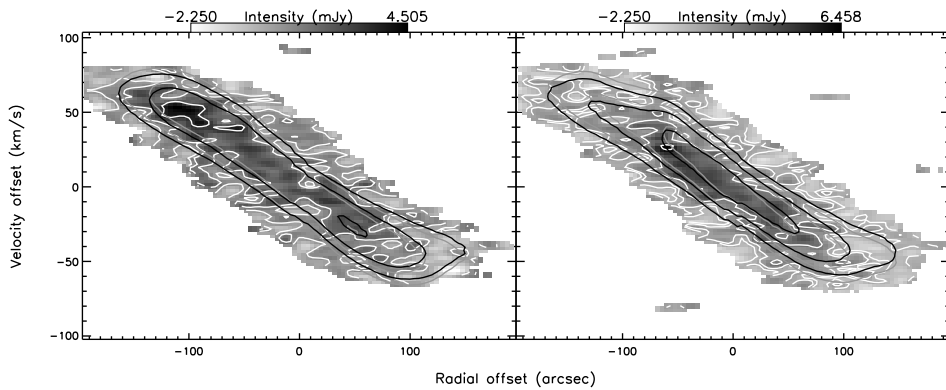


Figure 5.6: Two xv diagrams at $\pm 20\text{-}40''$ vertical offset (Right positive, Left negative) of the major axis. The color map and the black contours are the data. The white contours show the best fit model Model A with a lag = $5.3 \pm 0.8 \text{ km s}^{-1} \text{ kpc}^{-1}$. Red contours show the same model without a lag. With contour levels 1σ , 3σ , 7.5σ ($\sigma = 0. \text{ mJy}$). Color version on Page 140.

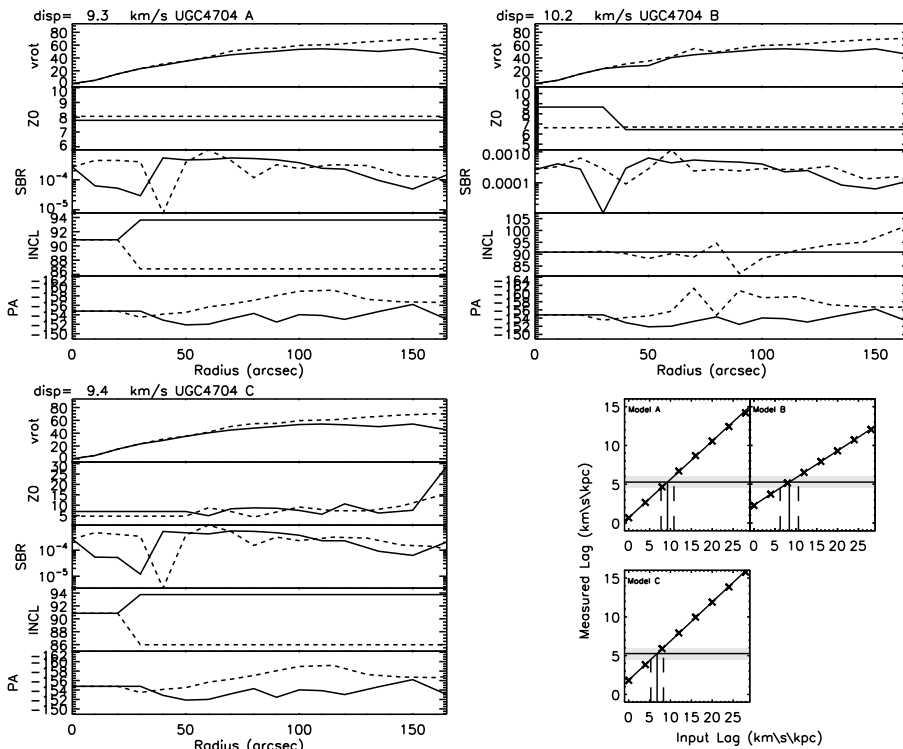


Figure 5.7: Same as Fig. 5.2 for UGC 4704

UGC 7321

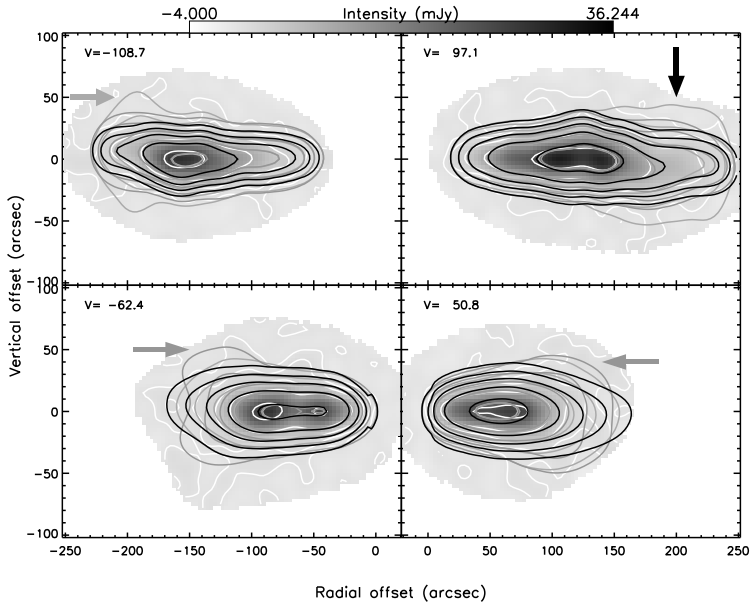


Figure 5.8: Four channel maps of UGC 7321. The velocities relative to the systemic velocity are shown in the top left corner of each panel. The color map and the white contours are the data. The red contours show the best fit model Model A. Green contours are a line of sight warp. Black contours are a flaring model. With contour levels 1σ , 3σ , 7.5σ , 18.75σ etc. ($\sigma = 0.5$ mJy). Color version on Page 141.

This galaxy shows the same behavior in its vertical distribution as UGC 1831. It is thought to have a lagging halo (Matthews & Wood 2003) but no vertical gradient could be quantified.

When we compare the fitted models to channel maps of the data (Figure 5.8) we see that indeed a flare (Model C, yellow contours) or a line of sight warp (Model B, green contours) does not match the data as well as a model without a flare or a line of sight warp. Both models show model channel maps that blow up in the vertical direction at large radii. For the warp this happens at velocities $\sim \pm 55$ km s $^{-1}$. This is indicated by the green arrows in Figure 5.8, bottom panels. In the top panels of Figure 5.8 we see the same behavior for the flaring model (black and yellow arrows). In this case this widening at large radii appears at higher velocities (~ 100 km s $^{-1}$). This behavior can not be recognized anywhere in the data channel maps. In general this galaxy is very similar to UGC 1831 but on smaller scales. Its vertical distribution would also be best fit by a double exponential as clearly can be seen in the top left panel of Figure 5.15.

When we measure the vertical gradient in the data we find that the extra-planar gas is lagging with 15.8 ± 4.2 km s $^{-1}$ kpc $^{-1}$. This measurement is confirmed when we compare PV diagrams parallel to the major axis of the data to the model (Figure 5.9). Here it is clearly seen that the model with a lag fits the data much better than a non-lagging

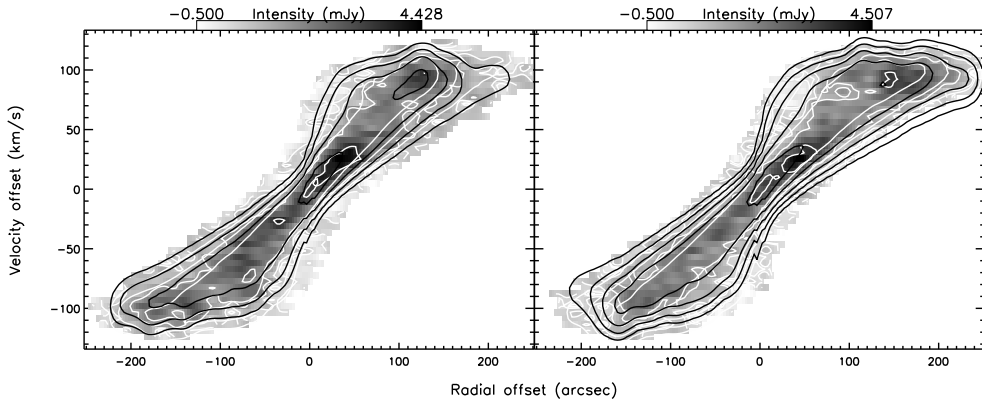


Figure 5.9: Two xv diagrams at $\pm 20\text{-}40''$ vertical offset (Right positive, Left negative) of the major axis. The color map and the black contours are the data. The red contours show the best fit model Model A lag = $15.8 \pm 4.2 \text{ km s}^{-1} \text{ kpc}^{-1}$. White contours the same model without a lag. With contour levels 1σ , 3σ , 7.5σ , 18.75σ etc. ($\sigma = 0.5 \text{ mJy}$). Color version on Page 141.

model.

UGC 7774

UGC 7774 is a special case in this sample as it is the only galaxy with an obvious warp. When we compare the channel maps of the HI data cube to the models it is seen that model B fits the data the best (Figure 5.11). This becomes even more clear when examining the two PV diagrams parallel to the minor axis shown in Figure 5.12. In this figure it can clearly be seen that the extra planar extensions do not occur at the right velocities in the case of Models A and C. This is pointed out by the black arrows in the plot.

When we measure the apparent lag of this galaxy (See Figure 5.7, little panels on the bottom right) we see that none of the models, be it lagging or not, fit the measurement from the data. This clearly indicates that our simplified best fit models are not an exact match to the data. This could be caused by the fact that we only consider a line of sight warp and a flaring model but not a combination of the two. However, the tremendous warp in UGC 7774 makes the measurements highly unstable. Therefore small differences between the model and the data will translate into huge differences in this measurement. Figure 5.13 shows the parameters for our best fitting models (Top panels, Bottom right panel). Here we can see how big the warp in this galaxy actually is. When we look at the values for the position angle we see that from the central parts to the last fitted ring there is a change in position angle of $\pm 30^\circ$. To investigate that this galaxy is not somehow lagging in addition to its gigantic warp we investigate the lagging models by eye. We find that including a lag to the model results in a less good representation of the data. We therefore conclude that this galaxy is not lagging and that the best fit model

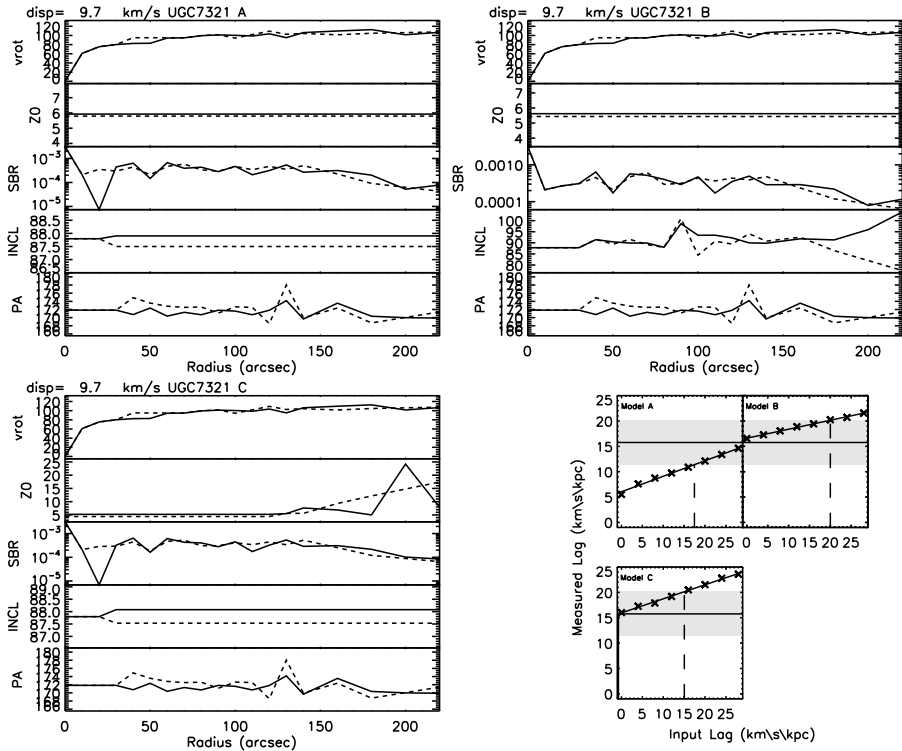


Figure 5.10: Same as Fig. 5.2 for UGC 7321

is Model B.

From the models we also obtain the rotation curve for each galaxy. These are shown in Figure 5.14 where the radius is in kpc to make a comparison between the different galaxies easier. The dashed rotation curves are at the approaching side whereas the solid lines are the rotation curves for the receding side of the galaxies. We use the average of these curves to determine the dynamical mass of each galaxy within the radius of their 25th magnitude contour in the B -band ($\frac{1}{2}D_{25}$). Also we determine the dynamical mass at the last point of the rotation curve. These masses and the radius of the last trustworthy point are listed in Table 5.5. This table also shows the total mass of the HI in each galaxy.

5.4 The structure of the halo

Besides obtaining a vertical velocity gradient for a galaxy one can also learn more about the halo by looking at the vertical distribution of the gas. Figure 5.15 shows the vertical HI profile for each galaxy. In this figure we also see the fits made to this profile to determine the scale height (dashed lines) from the data. UGC 0008 is an exception where

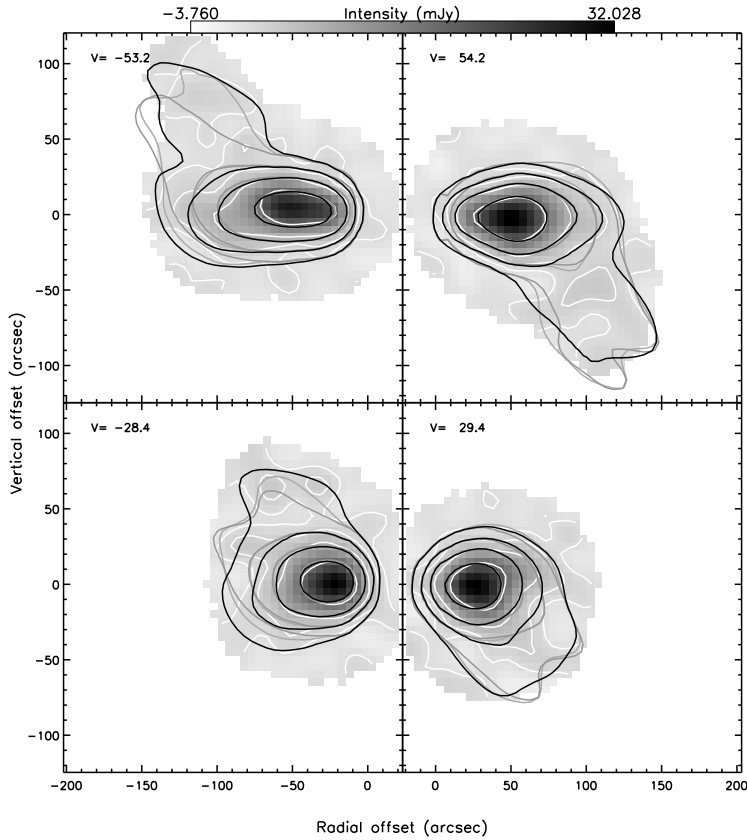


Figure 5.11: Four channel maps of UGC 7774. The velocities relative to the systemic velocity are shown in the top left corner of each panel. The color map and the white contours are the data. The red contours show the best fit model Model B. Green contours are a purely plane of the sky warp. Yellow contours are a flaring model. With contour levels 1σ , 3σ , 7.5σ , 18.75σ etc. ($\sigma = 0.94$ mJy). Color version on Page 142.

UGC No.	Dyn. mass M_{\odot}	Radius arcsec	Dyn. mass at D_{25} M_{\odot}	HI mass M_{\odot}
UGC 0008	1.9×10^{11}	240	1.5×10^{11}	1.3×10^9
UGC 1281	4.7×10^9	240	2.5×10^9	0.6×10^9
UGC 1831	1.3×10^{11}	400	1.3×10^{11}	4.2×10^9
UGC 4704	5.1×10^9	150	3.7×10^9	0.35×10^9
UGC 7321	1.7×10^{10}	220	1.1×10^{10}	0.28×10^9
UGC 7774	2.0×10^{10}	270	7.8×10^9	0.36×10^9

Table 5.5: Dynamical masses for the last measured point, the radius of the last measured point, Dynamical masses at $\frac{1}{2}D_{25}$ and the total HI mass.

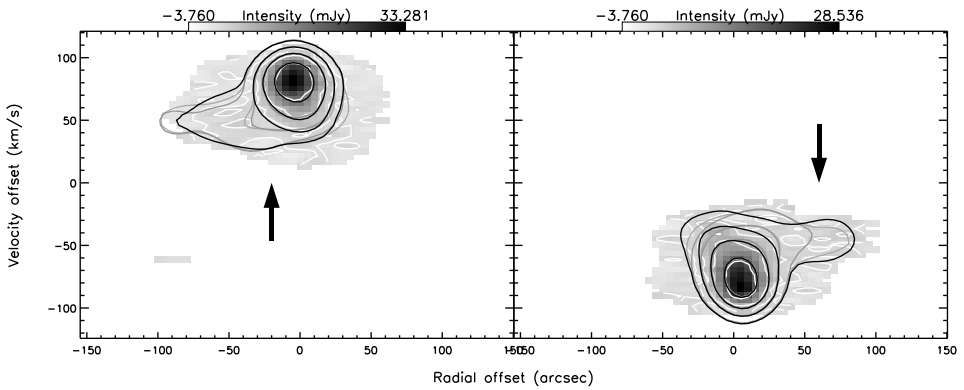


Figure 5.12: Two vy diagrams at $\pm 80''$ radial offset (Right positive, Left negative) of the minor axis. The color map and the white contours are the data. The red contours show the best fit model (Model B). Green contours are Model A. Yellow contours are a flare (Model C). With contour levels 1σ , 3σ , 7.5σ , 18.75σ etc. ($\sigma = 0.94$ mJy). The black arrows indicate where Model A and C deviate from the data. Color version on Page 141.

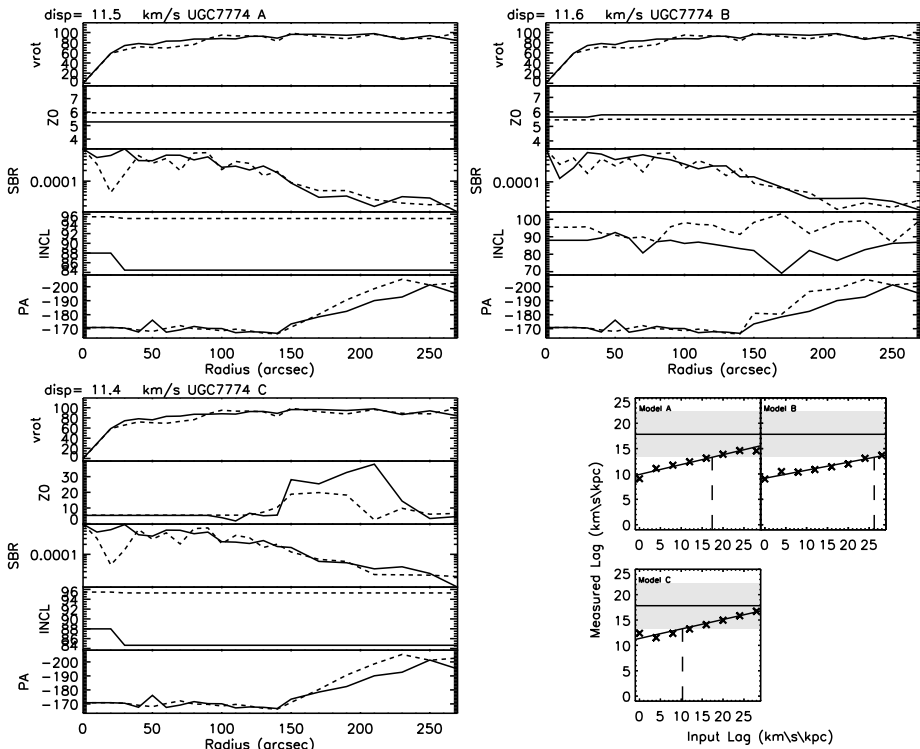


Figure 5.13: Same as Fig. 5.2 for UGC 7774.

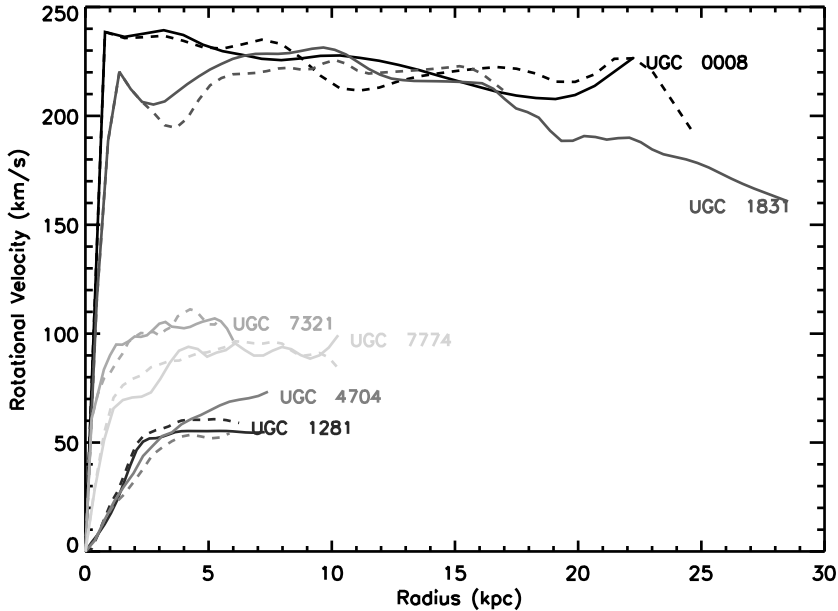


Figure 5.14: Rotation curves obtained from the fitting. Dashed line approaching side. Solid lines receding side. Color version on Page 142.

UGC No.	z_{data} (kpc)	z_{Model} (kpc)
UGC 0008	-	0.35
UGC 1281	-	0.2
UGC 1831	1.51	0.45
UGC 4704	0.28	0.3
UGC 7321	0.31	0.14
UGC 7774	1.15	0.21

Table 5.6: Scale heights for the six galaxies in our sample. z_{data} scale height measured from the data (See text). z_{Model} input scale height of the best fit model of each galaxy (See Table 5.4 and text)

there is no fit to the data because there is no indication for any gas outside the beam. UGC 1281 is also not fitted because even though there is clearly additional gas above and below the plane, the scale height is smaller than the beam and therefore difficult to measure. The average scale height above and below the plane for the other galaxies is shown in Table 5.6 together with the average scale heights of the best fit model.

In figure 5.15 it can be seen that all galaxies except UGC 1281 and UGC 0008 have a break in their vertical profiles. In UGC 7774 this break is caused by the warp but in the other galaxies it is most likely caused by a second component in the vertical distri-

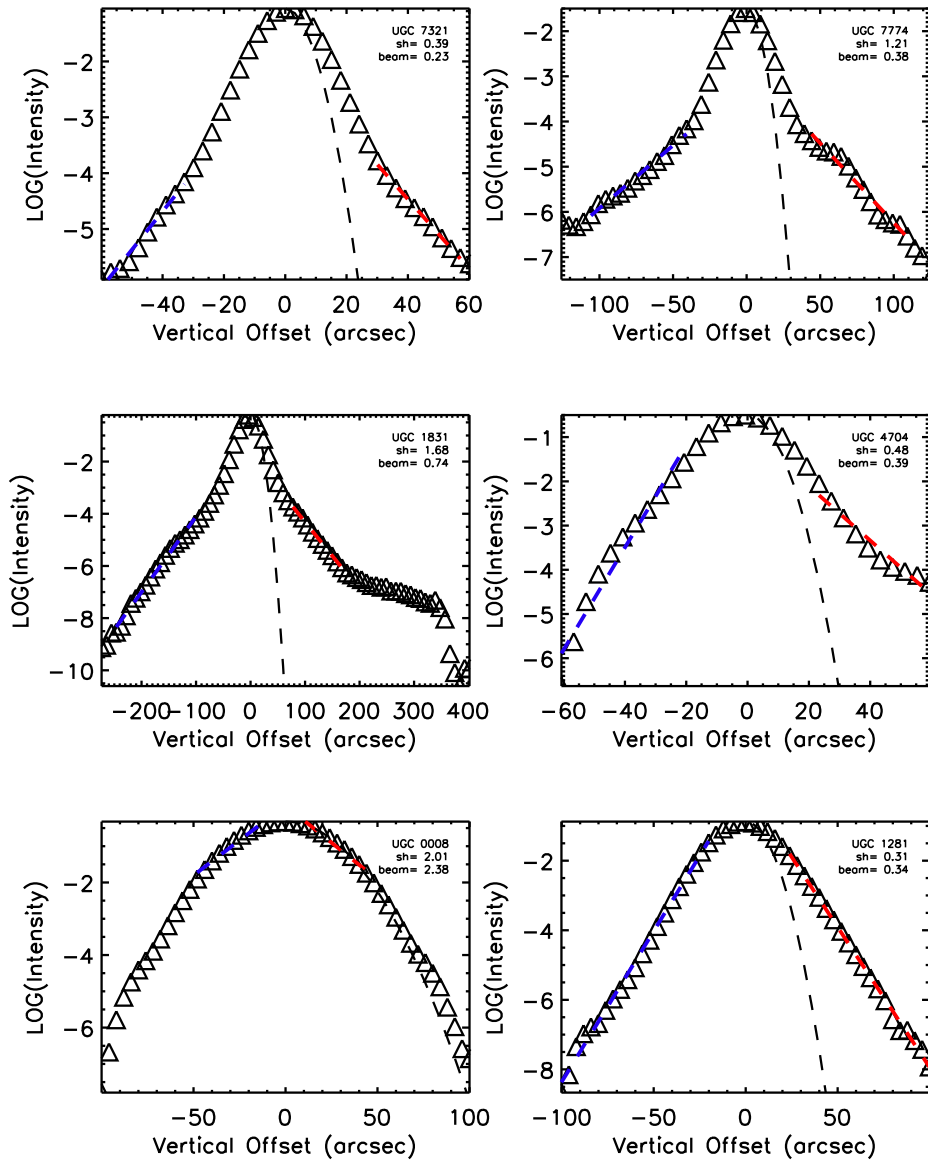


Figure 5.15: Vertical line profiles for the six galaxies. With on the left from top to bottom: UGC 7321, UGC 4704, UGC 0008. And on the right from top to bottom: UGC 7774, UGC 1831, UGC 1281. These are average line profiles of the inner part of the galaxies. The dashed lines indicate the beam size for each observation.

bution. We also see that the scale heights that TiRiFiC derives are much lower than the ones measured from the data by fitting an exponential to the slope. This is caused by the fact that TiRiFiC fits only a single exponential in the vertical direction and fits this exponential to the bright inner disk.

Now that we have obtained the vertical distribution and the lag of the galaxies in our sample we can correlate these with other properties of the galaxies in the sample.

The first thing we find from this small sample is that about 50% of our galaxies show a lag (See Table 5.4). This is by no means a complete or unbiased sample and so we will not obtain any general conclusion from this. However, it is interesting to see that the sample is split up in 3 distinct pairs of galaxies. These pairs are formed based on their mass and have one galaxy with a lagging halo and one with no lagging halo. The exception is the lowest mass pair with UGC 1281 since we cannot exclude a lagging halo in that galaxy.

When we compare the lags of the galaxies with their other properties such as mass, $24\mu\text{m}$ luminosity, and scale height, we find no obvious correlations. This is shown in Figure 5.16, where we plot the vertical gradient against other properties of the galaxies in our sample. The width of the ellipses in these plots indicate the error on the derived lag. The height is arbitrary except for the $24\mu\text{m}$ luminosities and the maximal rotational velocity where they indicate scaled versions of the errors. The panels in Figure 5.16 contain in addition to the galaxies from our sample also NGC 5775 and NGC 4302 (Open symbols in the plots). These two galaxies, in combination with UGC 1831, were studied by Heald et al. (2007), who found a weak correlation between the electron scale height and the vertical gradient of these galaxies. The electron scale height can be measured from the $\text{H}\alpha$ emission in a galaxy and is two times the scale height of the ionized gas. We were unable to obtain deep HI observations of these galaxies. Therefore these galaxies are not included in the correlation between the lag and HI mass or HI scale height. Their values for the dynamical mass and maximal rotational velocities are taken from Heald et al. (2007) and their $24\mu\text{m}$ luminosities are obtained in the same way as the rest of the sample. The upper left plot shows the obtained lag against the log of the total luminosity of a galaxy in $24\mu\text{m}$ from the Spitzer Space Telescope (See Table 5.3). For high $24\mu\text{m}$ fluxes the emission is a good tracer of the star formation rate of star forming regions in M 51 (Calzetti et al. 2005).

The upper right plot shows the obtained lag against the numerical Hubble type from the RC3 catalogue (de Vaucouleurs et al. 1992). The middle plots show the vertical gradient against the maximal rotational velocity (Right) and against the neutral gas scale heights (Left). The neutral gas scale height is an indicator of the extent of the gas halo, whereas the maximal rotational velocity is an indicator of the total mass of a galaxy.

The bottom plots show on the right the vertical gradient against dynamical mass determined at $\frac{1}{2}D_{25}$ and on the left the lag against the HI mass of each galaxy in our sample (See Table 5.5).

When we calculate the correlation coefficients for these distributions we find that all of the distributions have a correlation coefficient lower than 0.2. This is interesting in its own right because if the vertical gradient were determined by gas brought up from the plane of the galaxy, in processes related to star formation, a clear and obvious trend should be observed between the vertical gradient and the $24\mu\text{m}$ luminosity of a galaxy.

To complicate matters even more, a correlation between the electron scale height and the observed vertical gradient in a small sample of 3 galaxies (NGC 891, NGC 4302,

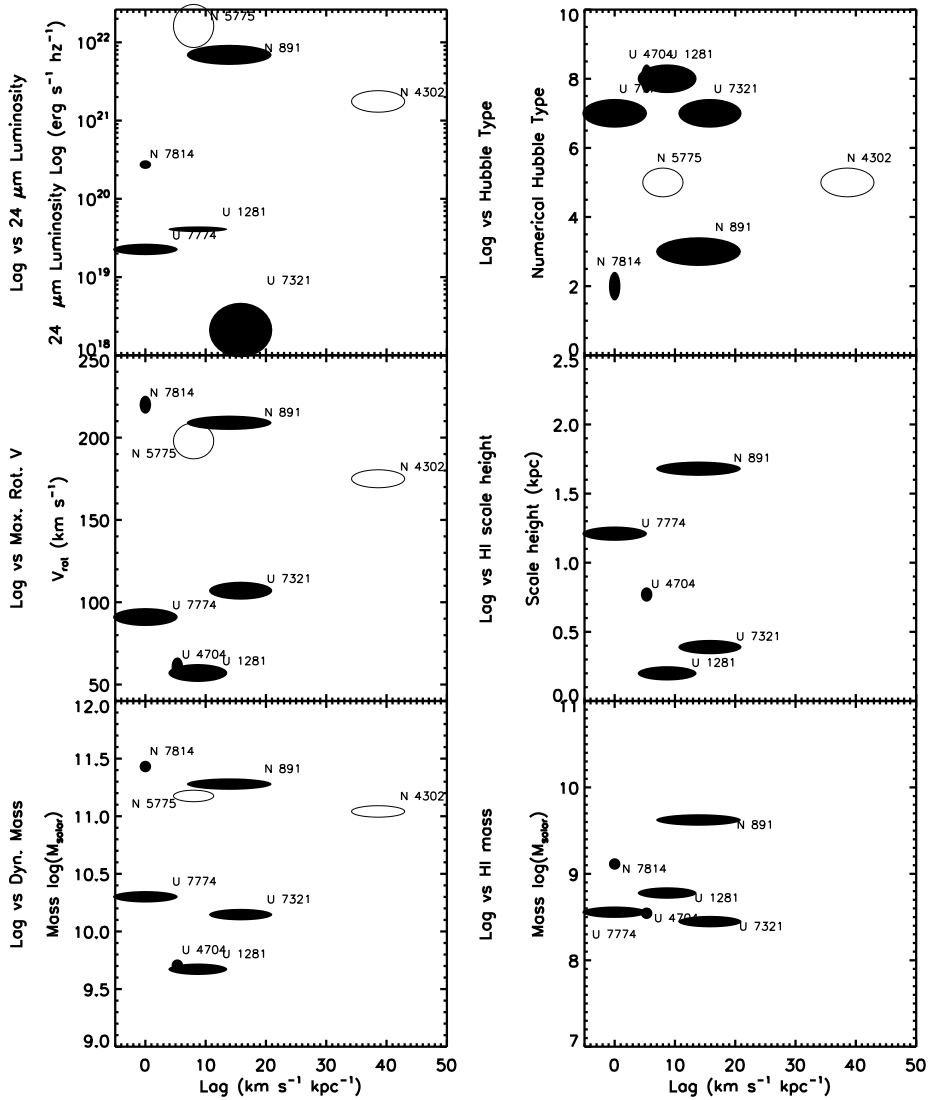


Figure 5.16: The obtained lags plotted against various masses, $24 \mu\text{m}$ luminosity and numerical Hubble type. With on the left the vertical gradient against from top to bottom $24\mu\text{m}$ luminosity, maximal rotation velocity and the dynamical mass at $\frac{1}{2}D_{25}$. On the right the vertical gradient against, from top to bottom, numerical Hubble type, HI scale height and HI mass. The width of the ellipses indicates the error in the lag and for the $24 \mu\text{m}$ and maximal rotational velocity the height indicates scaled version of the error

NGC 5775) was found by Heald et al. (2007). The electron scale height is correlated with the the star formation rate of a galaxy, and therefore their result implied that star formation is the most important factor in determining the vertical velocity gradient of disk galaxies. However, their sample only contained galaxies which are all of about equal mass. If we look at the lag vs $24 \mu\text{m}$ luminosity in Figure 5.16 (Top left panel) we see that this correlation would be reproduced if we only considered these three galaxies, but that it is destroyed by the extra galaxies in our sample.

The lack of any correlation in our sample implies that lagging halos are not dominated by one type of process. The lack of correlation with the SFR of a galaxy agrees with the underestimation of the vertical gradient by ballistic models. Of course there is always the possibility that the vertical gradient in the halos of galaxies is determined by a single process that is not considered here. However, it is unclear what such a process could be and it is much more likely that the gaseous halos, and therefore the vertical gradient, are created by a mixture of different possibilities such as the SFR and accretion combined

5.5 Summary and Future Work

We presented the analysis of the HI in a sample of 6 galaxies. These galaxies were modelled by fitting a tilted ring model to their data cubes with the program TiRiFiC. This was done in order to investigate the existence of lagging halos.

For these galaxies we find that 50% of them does have such a lagging halo. For two of them (UGC 1831 and UGC 7321) (Matthews & Wood 2003; Oosterloo et al. 2007) this was already known. For another dwarf galaxy (UGC 4704) this is a new measurement also we were able to quantify the vertical gradient in UGC 7321. We also find that of the six galaxies in our sample all of them contain some form of extra-planar gas (for UGC 0008 see Chapter 6). However, our sample is most likely biased towards galaxies with extra-planar gas due to the massive amount of observing time required.

We searched for possible correlations between the vertical gradient in a galaxy and other properties such as mass, SFR, vertical extent of the gas but found no significant ones. This implies that the creation of gaseous halos is not dominated by one of the processes investigated here. Therefore, they are created by either a mixture of SFR related processes and accretion or by a proces not considered in this Chapter.

To investigate these possibilities the sample should be extended. Also, for a more certain determination of the vertical gradient in edge-on galaxies TiRiFiC should fit lags and double exponentials to ensure all possible models for the galaxies. Especially because TiRiFiC now tries to compensate for the vertical gradient or second component in the vertical distribution by including either a line of sight warp or a flare when all parameters are left free to be fitted.